117 Stump, R. F., Robinson, K. R., Harold, R. L., and Harold, F. M., Endogenous electrical currents in the water mold *Blastocladiella emersonii* during growth and sporulation. Proc. natl Acad. Sci. (USA) *77* (1980) 6673–6677.
118 Telfer, W. H., Woodruff, R. I., and Huebner, E., Electrical polarity and cellular differentiation in meroistic ovaries. Am. Zoo. *21* (1981) 675–686.
119 Thornton, C. S., The relation of epidermal innervation to limb regeneration in *Amblystoma* larvae. J. exp. Zool. *127* (1954) 577–601.
120 Troxell, C. L., Scheffey, C., and Pickett-Heaps, J. D., Ionic currents during wall morphogenesis in *Micrasterias* and *Closterium*. Prog. clin. Biol. Res. *210* (1986) 105–112.
121 Verachtert, B., and DeLoof, A., Electrical fields around the polytrophic ovarian follicles of *Sarcophaga bullata* and the panoistic follicles of *Locusta migratoria*. Prog. clin. Biol. Res. *210* (1986) 173–180.
122 Waaland, S. D., and Lucas, W. J., An investigation of the role of transcellular ion currents in morphogenesis of *Griffithsia pacifica* Kylin. Protoplasma *123* (1984) 184–191.
123 Weisenseel, M. H., Control of differentiation and growth by endogenous electric currents, in: Biophysics, chap. 12, pp. 460–465. Eds W. Hoppe, W. Lohmann, H. Markl and H. Ziegler. Springer-Verlag, Berlin 1983.
124 Weisenseel, M. H., Dorn, A., and Jaffe, L. F., Natural H^+ currents traverse growing roots and root hairs of barley (*Hordeum vulgare* L.). Plant Physiol. *64* (1979) 512–518.
125 Weisenseel, M. H., and Jaffe, L. F., The major growth current through lily pollen tubes enters as K^+ and leaves as H^+. Planta *133* (1976) 1–7.
126 Weisenseel, M. H., and Kicherer, R. M., Ionic currents as control mechanism in cytomorphogenesis, in: Cytomorphogenesis in Plants, pp. 373–399. Ed. O. Kiermayer. Springer-Verlag, New York 1981.
127 Weisenseel, M. H., Nuccitelli, R., and Jaffe, L. F., Large electrical currents traverse growing pollen tubes. J. Cell Biol. *66* (1975) 556–567.
128 Wiley, L. M., and Nuccitelli, R., Detection of transcellular currents and effect of an imposed electric field on mouse blastomeres. Prob. clin. Biol. Res. *210* (1986) 197–204.
129 Winkel, G. K., and Nuccitelli, R., Strong ionic currents leave the midline of the 7.5 day postimplantation mouse embryo. J. Cell Biol. *105* (1987) 256a.
130 Woodruff, R. I., and Anderson, K. L., Nutritive cord connection and dye-coupling of the follicular epithelium to the growing oocytes in the telotrophic ovarioles in *Oncopeltus fasciatus*, the milkweed bug. Wilh. Roux Arch. *193* (1984) 158–163.
131 Woodruff, R. I., Huebner, E., and Telfer, W. H., Electrical properties of insect ovarian follicles: some challenges of a multicellular system. Prog. clin. Biol. Res. *210* (1986a) 147–154.
132 Woodruff, R. I., Huebner, E., and Telfer, W. H., Ion currents in *Hyalophora* Ovaries: the role of the epithelium and the intercellular spaces of the trophic cap. Devl Biol. *117* (1986b) 405–416.
133 Woodruff, R. I., and Telfer, W. H., Polarized intercellular bridges in ovarian follicles of the cecropia moth. J. Cell Biol. *58* (1973) 172–188.
134 Woodruff, R. I., and Telfer, W. H., Electrophoresis of proteins in intercellular bridges. Nature *286* (1980) 84–86.

0014-4754/88/080657-10$1.50 + 0.20/0

Prospects for NMR imaging in the study of biological morphogenesis

J. A. B. Lohman[a] and R. G. Ratcliffe*

[a] *Oxford Research Systems Limited, Nuffield Way, Abingdon, Oxon OX14 1RY (England), and Department of Plant Sciences, University of Oxford, Agricultural Science Building, Parks Road, Oxford OX1 3PF (England)*

Summary. Small objects can be visualised with a spatial resolution that approaches microscopic dimensions using the technique of high resolution nuclear magnetic resonance (NMR) imaging. Some important features of the method are described and the prospects for using the technique to study morphogenesis are discussed. It is concluded that NMR imaging, in conjunction with the related method of localised spectroscopy, is capable of producing novel structural information.
Key words. NMR; imaging techniques; morphogenesis; structural information; high resolution imaging.

Introduction

Many isotopes, some of them naturally abundant (e.g. ^1H, ^{31}P) and others not (e.g. ^{13}C, ^{15}N), have nuclear magnetic moments, and it is possible to detect such isotopes using the techniques of nuclear magnetic resonance (NMR). The phenomenon was first observed more than 40 years ago, and since that time NMR has developed into a versatile technique with many applications in physics, chemistry, biology and medicine. NMR detects transitions between the energy levels associated with the nuclear magnetic moments, and much of the success of the technique can be attributed to the fact that the measurable properties of these transitions depend on the molecular environment of the nucleus in a predictable way. Thus, NMR spectroscopy is arguably the most versatile technique for structural analysis in the chemistry laboratory[20], and it also finds many applications in biochemistry[40], for example in the characterisation of the structural and dynamic properties of macro-molecules in solution[58].

NMR techniques can be applied to living systems and the methods of particular interest are high resolution NMR spectroscopy and NMR imaging. In the spectroscopic approach, signals are detected from metabolites in the intracellular fluids and the metabolites are monitored under different physiological conditions[26]. Although the insensitivity of the technique limits it to metabolites present at relatively high concentrations, NMR spectroscopy has found many applications in vivo, including applications to mircroorganisms[6], plant tissues[48] and animal tissues[4,56]. The very small fraction of this work that has been concerned with developing systems (table) has concentrated on two areas: (i) the analytical problem of correlating changes in metabolite levels with the onset of developmental changes; and (ii) the role of intracellular

pH as a possible controlling factor in the regulation of development [12, 41].

Most of the work summarised in the table was done with collections of organisms at the same developmental stage, rather than with individuals, and the NMR spectra were averages over the total population. The conventional spectroscopic approach to living systems ignores the cellular heterogeneity of the sample and in so far as it is possible to obtain spatial information from such spectra, this information is usually at the level of identifying metabolic pools with particular spectroscopic properties [8]. This lack of spatial information is a disadvantage in studies of developing systems and it explains why NMR spectroscopy has been of only limited use in this area.

In contrast, NMR imaging exploits the heterogeneity of a sample to produce an image based on the spectroscopic properties of a bulk fraction distributed within the sample. In living systems, the bulk fraction is usually water and spatial information is encoded in the NMR signal by means of externally applied magnetic field gradients [39]. NMR imaging is well established as a clinical tool [33], but the clinical version of the technique, in which large objects are imaged at low spatial resolution, is unlikely to be of much interest to developmental biologists. However, recent developments in high resolution imaging, which enable small objects to be imaged with a spatial resolution that approaches cellular dimensions, together with the current trend towards combining the imaging and spectroscopic methods in various forms of localised spectroscopy [3] suggest that this situation is changing. These new methods for visualising developing systems non-invasively are reviewed here and their potential contribution to studies of morphogenesis is discussed.

Developmental changes investigated by NMR spectroscopy

Developmental change	Organism	NMR method	Observations
Sporulation	*Saccharomyces cerevisiae* (yeast)	^{13}C/labelling	Differences in the metabolism of [2-^{13}C]-acetate in sporulating and vegetatively growing cells [23]
Encystment	*Acanthamoeba castellanii* (protozoan)	$^{13}C/^{31}P$	Differences in the trehalose (^{13}C) and phosphonate (^{31}P) resonances between vegetative and encysted forms [21, 22]
Arousal from dormancy			
(a) Cysts	*Artemia salina* (brine shrimp)	^{31}P	Internal pH increased during arousal [10, 11]
	Artemia sp.	^{31}P	Diapause is not imposed by a fall in intracellular pH [24]
(b) Spores	*Pichia pastoris* (yeast)	^{13}C/labelling	Correlated trehalose metabolism and trehalase activity during dormancy and germination [5, 52]
	Phycomyces blakesleanus (fungus)	^{1}H	The breakdown of trehalose shortly after the start of germination coincided with an increase in the cytoplasmic water content and its mobility [54]
	Onoclea sensibilis (a fern)	^{31}P	Intracellular pH did not change during phytochrome-mediated germination [55]
(c) Seeds	Miscellaneous	$^{13}C/^{31}P$	Various changes in metabolite levels [14, 16, 19, 36]
Fertilisation and embryonic development			
(a) Sea urchins	Various	^{31}P	No change in intracellular pH on fertilisation [31]
	Strongylocentrotus purpuratus	^{31}P	Intracellular pH increased by 0.43 units on fertilisation [57]
(b) Amphibians	*Rana pipiens*	^{31}P	Transient increases in intracellular pH on removing metabolic blocks at first meiotic prophase and second meiotic metaphase [37, 38]
	R. pipiens	^{23}Na	Changes in the Na^+ signal during early development [29]
	Xenopus laevis	^{31}P	Intracellular pH increased by 0.24 units on fertilisation [42]
	X. laevis	^{31}P	Phosphorus metabolites monitored during development from the unfertilised egg to the feeding tadpole [15]
(c) Birds	Domestic fowl	^{31}P	Phosphorus metabolites monitored during development up to hatching [7]
Somatic embryogenesis			
	Medicago sativa (alfalfa) cultures	^{15}N/solid state	Compared the nitrogen utilisation in regenerating and non-regenerating cultures [51]
	M. sativa	^{31}P/solid state	Concluded that non-regenerating cultures were characterised by low intracellular pH [50]
Miscellaneous			
(a) Cell division cycle	*S. cerevisiae*	^{31}P	Transient intracellular pH rise following the addition of glucose to aerobic synchronous cultures arrested prior to 'start' [28]
(b) Differentiation	*Candida albicans* (fungus)	^{31}P	Changes in the polyphosphate signal during the dimorphic transition between yeast and mycelium [13]
	Dictyostelium discoideum (slime mold)	^{31}P	No pH difference between the pre-stalk and pre-spore cells during the initial stage of differentiation [32, 49]
	Friend leukemia cells	^{1}H	Marked increase in cytoplasmic phosphorylcholines during erythroid-like differentiation [1]
(c) Postnatal development	Rat brain	^{31}P	Changes in phosphorus metabolism between 10 and 20 days [43]

Imaging techniques

Imaging experiments on developing systems are likely to require the highest possible spatial resolution and this section begins with a discussion of the factors that limit the practicable resolution. Each data point in an NMR image corresponds to the signal from a volume element ('voxel') defined by the three orthogonal field gradients applied during the imaging experiment. The strength of the gradients in combination with the intrinsic frequency width of the NMR signal puts a theoretical limit on the spatial resolution, but in practice it is the sensitivity of the NMR experiment that is the limiting factor. There needs to be sufficient material within the voxel to give rise to a detectable NMR signal and as the voxel size is reduced so the signal strength decreases. For example, improving the spatial resolution by a factor of 2 in each dimension reduces the signal intensity by a factor of 8, implying a 64-fold increase in the total measurement time if the signal-to-noise ratio is to be maintained by performing time-averaging. Clearly time-averaging is a very inefficient method for improving the spatial resolution, and indeed it may well be impracticable when working with living systems because of the need to minimise the total imaging time to avoid image artifacts that arise from movements or changes in the specimen that are fast relative to the imaging time.

The solution to the sensitivity problem, and hence the key to high resolution imaging, is to operate at the highest possible field strength using a radio frequency (RF) circuit that is designed to optimise the signal from the sample. The signal strength increases with the strength of the polarising field and so, operating at the highest possible field is an effective route to high sensitivity. NMR magnets are currently available up to a field strength of 14 Tesla, corresponding to a ^{1}H resonance frequency of 600 MHz, and the only obstacle to exploiting the full range of field strengths for imaging purposes is the narrow bore of the highest field magnets. Thus for the foreseeable future, imaging at the highest spatial resolution is likely to be restricted to objects that can be accommodated within the confines of the RF and gradient coils within a 54-mm bore magnet, i.e. to objects, or parts of objects, with a diameter less than 1 cm. A further improvement in the sensitivity can be obtained by optimising the filling factor of the radio frequency resonator used to measure the NMR signal. A coil encompassing the specimen will normally produce an image of good quality and uniform appearance, but the size of the coil will limit the size of the object that can be imaged. Surface coils provide a more flexible alternative, but in this case the image intensity decreases with increasing distance from the coil and it is only possible to study structures within approximately one coil diameter of the surface.

The image of a *Xenopus laevis* egg in figure 1 gives some indication of the spatial resolution to be obtained in a high field 9.4 Tesla magnet[2]. The voxel volume is 32.5×10^{-15} m^3 (32.5 pl), with an in-plane ('pixel') resolution of 10×13 μm and a slice thickness of 250 μm. The ratio of the in-plane resolution to the slice thickness is largely under experimental control, but it should be borne in mind that a pixel resolution approaching a microscopic scale can only be obtained at the expense of a thick slice and that in multicellular systems this will lead to a decrease in the effective in-plane resolution. However, it should also be noted that the limit on the spatial resolution that can be achieved at the highest available field strengths has yet to be established.

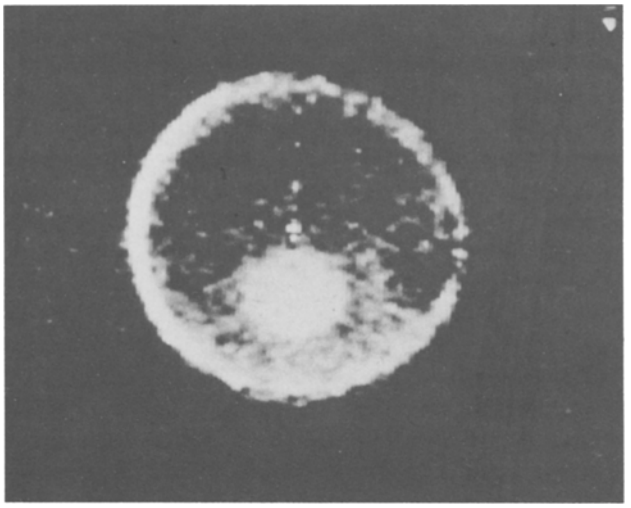

Figure 1. A 9.4 Tesla image of a transverse slice across a glass tube containing a stage 4 *X. laevis* ovum. The imaging conditions were: refocusing time, 16 ms; recycle time, 4 s; number of acquisition cycles, 4; total acquisition time, 32 min. The in-plane pixel resolution was 10×3 μm with a slice thickness of 250 μm. (Reproduced from Aguayo et al.[2])

The signal intensity in each pixel of figure 1 derives from the total ^{1}H magnetisation in the corresponding voxel. This microscopic magnetisation depends in part on the number of spins, i.e. ^{1}H nuclei, within the voxel but it also depends on the way in which the magnetisation is manipulated during the imaging experiment. Consequently, the signal strength is not a straightforward measure of the number of spins in a voxel – it would be incorrect, for example, to assume that the contrast in figure 1 arose solely from the variation in the water content within the egg – and so, care needs to be taken in the interpretation of image intensities. On the other hand, the ability to manipulate the magnetisation and thus to change the contrast in an image may lead to additional information about the sample.

The nuclear spin relaxation processes have an important bearing on the appearance of an image. For example, in order to obtain a two-dimensional image, the NMR signal has to be measured repetitively with different magnetic field gradient strengths and if the image is to reflect the spin density exactly, then it is essential to allow the magnetisation to return to equilibrium with the polarising field after each measurement. The equilibration pro-

cess is known as longitudinal relaxation and it is associated with a relaxation time, T_1, which depends on the molecular environment of the relaxing nucleus. If the repetition time (TR) for the NMR measurements is at least five times the T_1 for the slowest relaxing contributors to the magnetisation, then the image intensities will be directly related to the spin density, e.g. to the water content; whereas if the repetition time is shorter than 5 T_1, the more slowly relaxing contributors to the magnetisation will be saturated and their contribution to the image intensity will be reduced.

A second relaxation process, the transverse relaxation, is also important in the interpretation of NMR images because in many experiments, the magnetisation is detected by means of a spin-echo and the strength of the signal is weighted by the transverse relaxation of the magnetisation. This relaxation process describes the equilibration of the magnetisation in the plane perpendicular to the polarising field and it is characterised by a second relaxation time, T_2. The spin-echo can only be observed if the refocussing time for the echo (TE) is less than 5 T_2, and the shorter T_2 is in relation to TE, the weaker the echo. T_2, like T_1, is sensitive to the molecular environment of the relaxing nucleus and since T_2 is unlikely to be uniform throughout a heterogeneous object, it follows that the spatial dependence of the transverse relaxation of the magnetisation will influence the image intensity.

It is important to see the relaxation properties of a heterogeneous system as a potential source of new information, rather than as an obstacle to the measurement, for example, of the spatial dependence of the water content within the sample. Just as various stains can be used to highlight particular features in an optical micrograph, so the imaging conditions can be chosen to emphasise a particular component of the bulk magnetisation. For example, in living systems T_1 for water is usually longer than T_1 for lipids; whereas T_2 for water is usually shorter than T_2 for lipids. As a result, the relative contributions of the water and lipid signals to an image can be manipulated by adjusting either TR or TE: the lipid signal is favoured by increasing TE or reducing TR. Thus, by exploiting the intrinsic relaxation differences within a tissue it is possible to control the contrast within the image and this can lead to more detailed information about the tissue.

One further aspect of image interpretation needs to be mentioned here and this concerns the complications that can arise when the bulk magnetisation is derived from more than one chemical species. The ^1H magnetisation of a tissue is often dominated by the water content, but in some cases the NMR signal may originate from two major fractions, e.g. water and lipid, with different chemical shift values. In this situation the image constructed from the total magnetisation is actually the superposition of two images derived from the two main contributors to the magnetisation and the effect of the frequency difference between the two resonances is to displace one image relative to the other. If the frequency difference is small relative to the gradient strength, then the displacement is negligible and the image will not be noticeably flawed; whereas if the frequency difference is large, the displacement will be significant and it may be possible to exploit

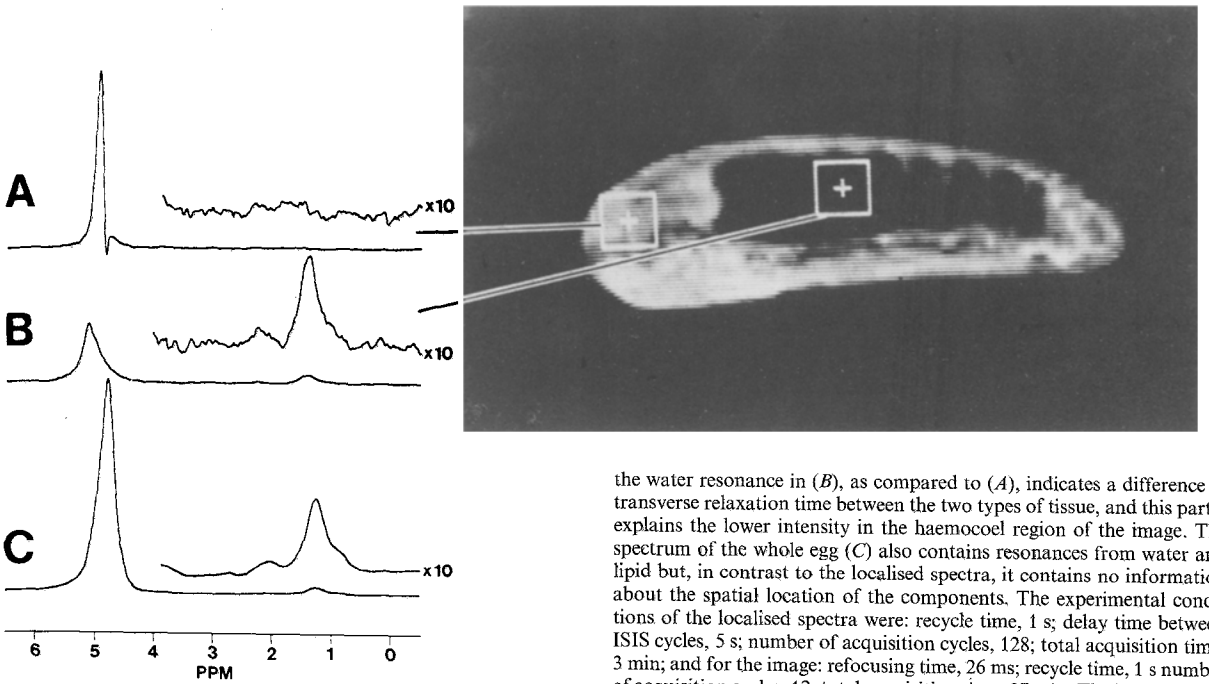

Figure 2. 4.7 Tesla ISIS spectra[44] from a locust egg at 77% development showing that the volume dorsal to the stomatodeum (*A*) is essentially void of lipid while the haemocoel (*B*) contains lipid. The larger line width for the water resonance in (*B*), as compared to (*A*), indicates a difference in transverse relaxation time between the two types of tissue, and this partly explains the lower intensity in the haemocoel region of the image. The spectrum of the whole egg (*C*) also contains resonances from water and lipid but, in contrast to the localised spectra, it contains no information about the spatial location of the components. The experimental conditions of the localised spectra were: recycle time, 1 s; delay time between ISIS cycles, 5 s; number of acquisition cycles, 128; total acquisition time, 3 min; and for the image: refocusing time, 26 ms; recycle time, 1 s number of acquisition cycles, 12; total acquisition time, 27 min. The in-place pixel resolution in the image was 100 × 100 μm with a slice thickness of 500 μm and the localised spectra were obtained from cubic volumes of 500 × 500 × 500 μm. (Reproduced from Gassner and Lohman[27])

the phenomenon to obtain separate images of the different chemical species[34]. An important point is that the frequency difference between the two resonances increases linearly with the strength of the polarising field and so chemical shift effects are likely to be particularly important in high resolution imaging experiments at high magnetic field strengths. Suppressing these effects in high resolution images requires the use of strong gradients to satisfy the condition that the frequency difference should be small relative to the gradient strength.

Methods for combining imaging techniques with the spectroscopic approach to yield localised spectra are currently being developed in many laboratories, but the extent to which these methods will be useful at a microscopic scale is uncertain. The only relevant study so far achieved a reasonable signal-to-noise ratio for the water and lipid resonances from a volume of 125×10^{-12} m^3 (125 nl), corresponding to 25 voxels in the high resolution image[27] (fig. 2). The use of water and lipid suppression sequences and improvements in the localisation technique itself may greatly enhance the sensitivity of the method to the point at which it may be possible to obtain localised spectra from some tissue metabolites. A metabolite at the high concentration of 10 mM is 10,000 times more dilute than the tissue water protons and so it is clear that the spatial resolution in a localised spectrum will be considerably less than in a simple image. Recent localised spectra obtained in a whole body magnet have shown that good quality ^{1}H spectra can be obtained from a few ml of brain tissue in the head[30] and results have also been obtained with the less sensitive ^{31}P nucleus that suggest that localised ^{31}P spectra can be obtained from volumes of the order of 30 ml. These localised spectra were obtained from volumes corresponding to a few hundred voxels in the simple image, and extrapolating from these results to the microscopic scale of high resolution imaging suggests that it may be possible to obtain localised spectra from volumes of between 10^{-9} and 10^{-12} m^3. However, it should be noted that an experimental demonstration of this prediction has yet to be made.

Discussion

NMR imaging is a source of structural information and its non-invasive character makes it particularly suitable for investigating systems in which the structure changes. For example, figure 3 shows a set of high resolution images obtained from a germinating mung bean (*Phaseolus aurens*) seed, and it is clear that the emergence of the root and the development of structure within the cotyledon can be followed[17]. The potential of high resolution imaging for studying developmental processes has been explored more fully in an investigation of the embryonic development of the desert locust (*Schistocerca gregaria*)[27]. Images of the egg revealed the formation of

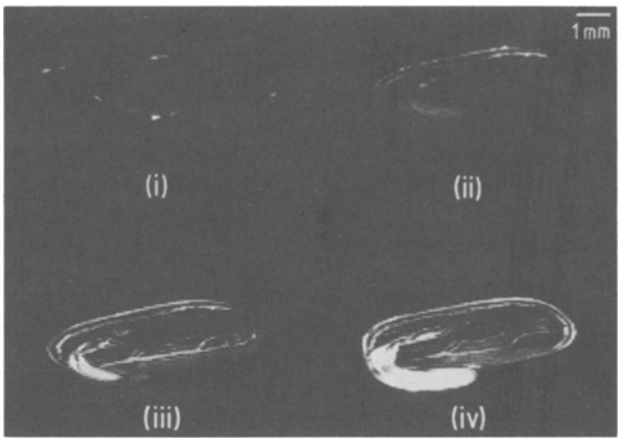

Figure 3. 4.7 Tesla images of a germinating mung bean taken (i) 2, (ii) 17.5, (iii) 29, and (iv) 44 h after the start of germination. The imaging plane was parallel to the plane of the cotyledons and the slice displayed is centred approximately on the embryonic axis. The imaging conditions used were: refocusing time, 22 ms; recycle time, 1.52 s; number of acquisition cycles, 16; total acquisition time, 52 min. The in-plane pixel resolution was 70 × 70 μm with a slice thickness of 590 μm. (Reproduced from Connelly et al.[17])

anatomical structures and embryonic movements during the development from fertilisation to hatching.

When comparing the images in figures 1 and 3 with conventional optical micrographs, it is important to remember that the physical origin of the contrast detected by the two techniques is different. Optical methods highlight the dense, opaque structures within a thin section; whereas NMR imaging highlights the regions in between these structures, since it is the liquid phase of the object that contributes to the detected magnetisation. The resolution in an NMR image is less good than in an optical section, but this shortcoming has to be set against the ability of the technique to follow structural changes within a fully functional organism and the fact that the structural information content is different. Clearly, the two techniques are complementary and by drawing on the microscopic approach to identify the locations highlighted by the NMR method, it should be possible to extend the interpretation of the images.

The locust study emphasises the way in which imaging methods can be used to monitor the chemical composition of the egg during development[27]. It was possible, for example, to image the water and lipid distribution separately (fig. 4) and thus to show that the lipid distribution in the yolk was not necessarily uniform. It was also possible to record localised spectra (fig. 2) and to show that the water content of the yolk remained constant during development. As indicated in the previous section, significant improvements are likely in the techniques of localised spectroscopy but even at the present level of sensitivity and spatial resolution it is possible to obtain new information about the bulk fractions in developing systems.

Image intensities also depend on the relaxation behaviour of the system and experiments can be devised to

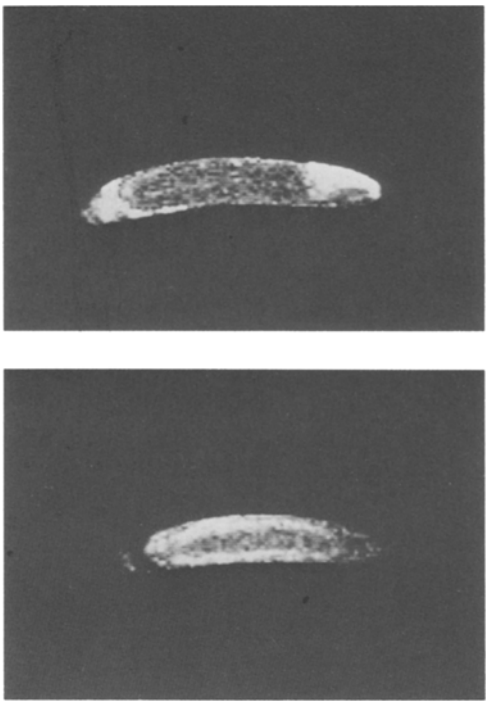

Figure 4. 4.7 Tesla images of a locust egg showing (*A*) the water distribution and (*B*) the lipid distribution in a mid-saggital slice at 22% development. The imaging conditions used were the same as for fig. 2; the refocusing time for the lipid image (*B*) was 46 ms. (Reproduced from Gassner and Lohman [27])

measure the spatial dependence of the relaxation times. This type of measurement is a potential source of information about the physical nature of localised regions within a heterogeneous system since the relaxation times can be influenced by many different factors, including molecular mobility, the viscosity of the medium, interactions with paramagnetic ions, macromolecules and surfaces, exchange processes and diffusion phenomena. Water relaxation measurements have been used extensively to investigate the properties of tissue water fractions [35], but the interpretation of the results has often been limited by the spatial complexity of the samples [8]. Combining relaxation measurements with imaging procedures will reduce the uncertainty inherent in the interpretation of the simple relaxation data, and indeed the feasibility of this approach has recently been demonstrated by an investigation of the spatial dependence of the water diffusion rate in a wheat grain [25]. In a developmental context, localised relaxation measurements offer the prospect of correlating changes in viscosity or mobility with the onset or cessation of metabolic functions.

If high resolution imaging proves to be a useful technique for studying morphogenesis, then it will be necessary to assess the extent to which the technique itself can interfere with developmental processes. Tissues respond in various ways to static magnetic fields, time-dependant magnetic fields and radiofrequency fields [9] and much effort is being directed into the potential clinical hazards of imaging procedures [39, 47]. No adverse effects of the technique have been observed so far, but this conclusion has little relevance to the use of high resolution imaging proposed here because: (i) very little work has been done with developing systems; and (ii) no results of any kind have been reported under the conditions of a high resolution imaging experiment, i.e. under conditions of very high static and gradient field strengths. Less extreme conditions caused no effects on bacterial growth [53], lymphocyte cell division [18] and the early stages of amphibian development [46], but there is no reliable means of extrapolating from these results to the conditions of a high resolution imaging experiment and thus no substitute for a programme of control experiments at high static and gradient field strengths.

The high gradient strengths are the most likely source of difficulty: a changing magnetic field generates a voltage and the rapid switching of the gradient in a high resolution imaging experiment is likely to cause appreciable current densities even in small sample volumes. For example, reversing a gradient of 0.5 T/m^{-1} in a switching time of 1 ms could cause a current density of 2.5 mA/m^{-2} around the circumference of a spherical object with a diameter of 1 cm [9]. This figure is comparable with the current densities that are associated with developmental processes [45] and although the rapidly varying polarity of the induced currents may well ensure that the technique is harmless, it underlines the need for a critical evaluation of the non-invasive nature of the imaging technique in its high resolution form.

Conclusion

High resolution imaging is in its infancy but it has progressed to the point where it is capable of generating novel structural information about biological systems. It provides a new way of visualising changes that occur during morphogenesis, and it is to be hoped that developmental biologists will have the opportunity to exploit the technique as the equipment for high resolution imaging becomes more widely available.

* Present address: Philips Medical Systems, MR Physics, P.O. Box 10 000, Best (The Netherlands)

1 Agris, P. F., and Campbell, I. D., Proton nuclear magnetic resonance of intact friend leukemia cells: phosphorylcholine increase during differentiation. Science *216* (1982) 1325–1327.

2 Aguayo, J. B., Blackband, S. J., Schoeniger, J., Mattingly, M. A., and Hintermann, M., Nuclear magnetic resonance imaging of a single cell. Nature *322* (1986) 190–191.

3 Aue, W. P., Localisation methods for *in vivo* nuclear magnetic resonance spectroscopy. Rev. magn. Reson. Med. *1* (1986) 21–72.

4 Avison, M. J., Hetherington, H. P., and Shulman, R. G., Applications of NMR to studies of tissue metabolism. A. Rev. Biophys. Biophys. Chem. *15* (1986) 377–402.

5 Barton, J. K., Den Hollander, J. A., Hopfield, J. J., and Shulman, R. G., ^{13}C nuclear magnetic resonance study of trehalose mobilisation in yeast spores. J. Bact. *151* (1982) 177–185.

6 Baxter, R. L., Microbiological applications of NMR spectroscopy. Microbiol. Sci. *2* (1985) 203–211; 340–345.

7 Belton, P. S., Gordon, R. E., Jones, J. M., and Shaw, D., A ^{31}P topical magnetic resonance study of embryonic development in hens' eggs. Br. Poul. Sci. *24* (1983) 429–433.

8 Belton, P. S., and Ratcliffe, R. G., NMR and compartmentation in biological tissues. Prog. NMR Spec. *17* (1985) 241–279.

9 Budinger, T. F., Thresholds for physiological effects due to rf and magnetic fields used in NMR imaging. IEEE Trans. Nucl. Sci. NS-26 (1979) 2821–2825.

10 Busa, W. B., and Crowe, J. H., Intracellular pH regulates transitions between dormancy and development of brine shrimp (*Artemia salina*) embryos. Science *221* (1983) 366–368.

11 Busa, W. B., Crowe, J. H., and Matson, G. B., Intracellular pH and the metabolic status of dormant and developing *Artemia* embryos. Archs Biochem. Biophys. *216* (1982) 711–718.

12 Busa, W. B., and Nuccitelli, R., Metabolic regulation via intracellular pH. Am. J. Physiol. *246* (1984) R409–R438.

13 Cassone, A., Carpinelli, G., Angiolella, L., Maddaluno, G., and Podo, F., ^{31}P nuclear magnetic resonance study of growth and dimorphic transition in *Candida albicans*. J. gen. Microbiol. *129* (1983) 1569–1575.

14 Chen, S., Elofson, R. M., and MacTaggart, J. M., Carbon-13 nuclear magnetic resonance studies of lipids and starch digestion in intact seeds. J. Agric. Food Chem. *27* (1979) 435–438.

15 Colman, A., and Gadian, D. G., ^{31}P nuclear magnetic resonance studies on the developing embryos of *Xenopus laevis*. Eur. J. Biochem. *61* (1976) 387–396.

16 Colnago, L. A., and Seidl, P. R., Application of carbon-13 nuclear magnetic resonance to the germination of soybean seeds in vivo. J. Agric. Food Chem. *31* (1983) 459–461.

17 Connelly, A., Lohman, J. A. B., Loughman, B. C., Quiquampoix, H., and Ratcliffe, R. G., High resolution imaging of plant tissues by NMR. J. exp. Bot. *38* (1987) 195.

18 Cooke, P., and Morris, P. G., The effects of NMR exposure on living organisms. 2 A genetic study of human lymphocytes. Br. J. Radiol. *54* (1981) 622–625.

19 Delfini, M., Angelini, R., Bruno, F., Conti, F., Di Cocco, E., Giuliani, A. M., and Manes, F., Phosphate metabolites in germinating lettuce seeds observed by ^{31}P NMR spectroscopy. Cell molec. Biol. *31* (1985) 385–389.

20 Derome, A. E., Modern NMR techniques for chemistry research. Pergamon Press, Oxford 1987.

21 Deslauriers, R., Byrd, R. A., Jarrell, H. C., and Smith, I. C. P., ^{31}P NMR studies of vegetative and encysted cells of *Acanthamoeba* castellanii. Observation of phosphonic acids in live cells. Eur. J. Biochem. *111* (1980) 369–375.

22 Deslauriers, R., Jarrell, H. C., Byrd, R. A., and Smith, I. C. P., Observation by ^{13}C NMR of metabolites in differentiating amoeba. Trehalose storage in encysted *Acanthamoeba castellanii*. FEBS Lett. *118* (1980) 185–190.

23 Dickinson, J. R., Dawes, I. W., Boyd, A. S. F., and Baxter, R. L., ^{13}C NMR studies of acetate metabolism during sporulation of *Saccharomyces cerevisiae*. Proc. natl Acad. Sci. USA *80* (1983) 5847–5851.

24 Drinkwater, L. E., and Crowe, J. H., Regulation of embryonic diapause in *Artemia*: environmental and physiological signals. J. exp. Zool. *241* (1987) 297–307.

25 Eccles, C. D., Callaghan, P. T., and Jenner, C. F., Biophys. J. (1987) submitted for publication.

26 Gadian, D. G., Nuclear magnetic resonance and its applications to living systems. Clarendon Press, Oxford 1982.

27 Gassner, G., and Lohman, J. A. B., Combined proton NMR imaging and spectral analysis of locust embryonic development. Proc. natl Acad. Sci. USA *84* (1987) 5297.

28 Gillies, R. J., Ugurbil, K., Den Hollander, J. A., and Shulman, R. G., ^{31}P NMR studies of intracellular pH and phosphate metabolism during cell division cycle of *Saccharomyces cerevisiae*. Proc. natl Acad. Sci. USA *78* (1981) 2125–2129.

29 Gupta, R. K., Kostellow, A. B., and Morrill, G. A., NMR studies of intracellular sodium ions in amphibian oocytes, ovulated eggs and early embryos. J. biol. Chem. *260* (1985) 9203–9208.

30 Hanstock, C. G., Rothman, D. L., Jue, T., and Shulman, R. G., J. magn. Reson. (1988) submitted for publication.

31 Inoue, H., and Yoshioka, T., Measurement of intracellular pH in sea urchin eggs by ^{31}P NMR. J. cell. Physiol. *105* (1980) 461–468.

32 Kay, R. R., Gadian, D. G., and Williams, S. R., Intracellular pH in *Dictyostelium*: a ^{31}P nuclear magnetic resonance study of its regulation and possible role in controlling cell differentiation. J. Cell Sci. *93* (1986) 165–179.

33 Kean, D. M., and Smith, M. A., Magnetic resonance imaging. Principles and applications. William Heinemann Medical Books, London 1986.

34 Lohman, J. A. B., Orddige, R. J., and Connelly, A., Spin echo imaging of multiple chemical shifts. Magn. Reson. Med. *5* (1987) 83 (and references quoted therein).

35 Mathur-de Vre, R., The NMR studies of water in biological systems. Prog. Biophys. molec. Biol. *35* (1979) 103–134.

36 McCain, D. C., ^{31}P NMR study of turnip seed germination and sprout growth inhibition by peroxydisulphate ion. Biochim. biophys. Acta *763* (1983) 231–236.

37 Morrill, G. A., Kostellow, A. B., Mahajan, S., and Gupta, R. K., Role of calcium in regulating intracellular pH following the stepwise release of the metabolic blocks at first meiotic prophase and second meiotic metaphase in amphibian oocytes. Biochim. biophys. Acta *804* (1984) 107–117.

38 Morrill, G. A., Weinstein, S. P., Kostellow, A. B., and Gupta, R. K., Studies of insulin action on the amphibian oocyte plasma membrane using NMR, electrophysiological and ion flux techniques. Biochim. biophys. Acta *844* (1985) 371–392.

39 Morris, P. G., Nuclear magnetic resonance imaging in medicine and biology. Clarendon Press, Oxford 1986.

40 Moore, G. R., Ratcliffe, R. G., and Williams, R. J. P., NMR and the biochemist. Essays Biochem. *19* (1983) 142–195.

41 Nuccitelli, R., and Heiple, J. M., Summary of the evidence and discussion concerning the involvement of pH_i in the control of cellular functions, in intracellular pH: its measurement, regulation and utilisation in cellular functions, pp. 567–586. Eds R. A. Nuccitelli and D. W. Deamer. A.R. Liss Inc., New York 1982.

42 Nuccitelli, R., Webb, D. J., Lagier, S. T., and Matson, G. B., ^{31}P NMR reveals increased intracellular pH after fertilization in *Xenopus* eggs. Proc. natl Acad. Sci. USA *78* (1981) 4421–4425.

43 Ogawa, S., Lee, T. M., and Glyn, P., Energy metabolism in rat brain *in vivo* studied by ^{31}P nuclear magnetic resonance: changes during postnatal development. Archs Biochem. Biophys. *248* (1986) 43–45.

44 Orddige, R. J., Connelly, A., and Lohman, J. A. B., Image-selected *in vivo* spectroscopy (ISIS). A new technique for spatially selective NMR spectroscopy. J. magn. Reson. *66* (1986) 283–294.

45 Overall, R., and Jaffe, L. F., Patterns of ionic current through *Drosophila* follicles and eggs. Devl Biol. *108* (1985) 102–119.

46 Prasad, N., Wright, D. A., and Forster, J. D., Effects of nuclear magnetic resonance on early stages of amphibian development. Magn. Reson. Imag. *1* (1982) 35–37.

47 Prato, F. S., Ossenkopp, K. P., Kavaliers, M., Sestine, E., and Teskey, G. C., Attenuation of morphine-induced analgesia in mice by exposure to magnetic resonance imaging: separate effects of the static, radiofrequency and time-varying magnetic fields. Magn. Reson. Imag. *5* (1987) 9–14.

48 Ratcliffe, R. G., Application of nuclear magnetic resonance methods to plant tissues. Meth. Enzymol. *148* (1987) 683–700.

49 Satre, M., Klein, G., and Martin, J. B., Intracellular pH control in *Dictyostelium discoideum*: a ^{31}P NMR analysis. Biochimie *68* (1986) 1253–1261.

50 Schaefer, J., Regeneration in alfalfa tissue culture. Characterisation of intracellular pH during somatic embryo production by solid state ^{31}P NMR. Plant Physiol. *79* (1985) 584–589.

51 Skokut, T. A., Manchester, J., and Schaefer, J., Regeneration in alfalfa tissue culture. Stimulation of somatic embryo production by amino acids and N-15 NMR determination of nitrogen utilisation. Plant Physiol. *79* (1985) 579–583.

52 Thevelein, J. M., Den Hollander, J. A., and Shulman, R. G., Changes in the activity and properties of trehalase during early germination of yeast asco spores. Correlation with trehalose breakdown as studied by *in vivo* ^{13}C NMR. Proc. natl Acad. Sci. USA *79* (1982) 3503–3507.

53 Thomas, A., and Morris, P. G., The effects of NMR exposure on living organisms. 1 A microbial assay. Br. J. Radiol. *54* (1981) 615–621.

54 Van Laere, A., Francois, A., Overloop, K., Verbeke, M., and Van Gerven, L., Relation between germination, trehalose and the status of water in *Phycomyces blakesleeanus* spores as measured by proton NMR. J. gen. Microbiol. *133* (1987) 239–245.

55 Wayne, R., Rice, D., and Hepler, P. K., Intracellular pH does not change during phytochrome-mediated spore germination in *Onoclea*. Devl Biol. *113* (1986) 97–103.

56 Williams, S. R., and Gadian, D. G., Tissue metabolism studied in vivo by nuclear magnetic resonance. J. exp. Physiol. *71* (1986) 335–360.

57 Winkler, M. M., Matson, G. B., Hershey, J. W. B., and Bradbury, E. M., ^{31}P NMR study of the activation of the sea urchin egg. Exp. Cell Res. *139* (1982) 217–222.

58 Wuethrich, K., NMR of proteins and nucleic acids. Wiley, New York 1986.

0014-4754/88/080666-07$1.50 + 0.20/0